A Novel Discrete-time Nonlinear Model Predictive Control Based on State Space Model

Carlos Sotelo, Antonio Favela-Contreras*, Francisco Beltrán-Carbajal, Graciano Dieck-Assad, Pedro Rodríguez-Cañedo, and David Sotelo

International Journal of Control, Automation and Systems 16(6) (2018) 2688-2696

ISSN:1598-6446 (print version)
eISSN:2005-4092 (electronic version)

To link to this article:
http://dx.doi.org/10.1007/s12555-018-0041-x

Springer

International Journal of Control, Automation and Systems 16(6) (2018) 2688-2696
http://dx.doi.org/10.1007/s12555-018-0041-x
ISSN:1598-6446 eISSN:2005-4092
http://www.springer.com/12555

A Novel Discrete-time Nonlinear Model Predictive Control Based on State Space Model

Carlos Sotelo, Antonio Favela-Contreras*, Francisco Beltrán-Carbajal, Graciano Dieck-Assad, Pedro Rodríguez-Cañedo, and David Sotelo

Abstract: This paper proposes a novel finite dimensional discrete-time Nonlinear Model Predictive Control. This technique is based on discrete-time state-space models, Taylor series expansion for prediction and performance index optimization. Furthermore, the technique extends the concept of the Lie derivative for the discrete time case using Euler backwards method. The performance validation for the discrete-time Nonlinear Model Predictive Control uses the simulation of a single-link flexible joint robot and the inverted pendulum. Comparison of the proposed finite dimensional discrete-time Nonlinear Model Predictive Control technique with Feedback Linearization Control is also discussed. Analytical and numerical results show excellent performances for both, the single-link flexible joint and inverted pendulum controllers using the proposed discrete-time Nonlinear Model Predictive Control technique.

Keywords: Feedback linearization, Lie derivatives, nonlinear model predictive control, relative degree.

1. INTRODUCTION

Nonlinear control techniques are mature and well-established methodologies for designing controllers in different engineering areas such as advanced manufacturing, energy, environment, health, aerospace, etc. They are based on the linearizing model process around equilibrium points and a nonlinear controller is generally used to solve constrained optimization control problems [1–3]. However, when the process presents high nonlinearities, the controller performance decreases or stabilization becomes infeasible. Several nonlinear control techniques are used to overcome these problems [4–6]. For instance, in feedback linearization control (FLC) the nonlinearities are cancelled and a desired linear dynamic is used as a performance index [7, 8]. Also, sliding mode control (SMC), that is widely-employed technique in nonlinear control, is a particular type of variable structure control systems (VSCS) where the VSCS is designed to drive and then constrain the system state to lie within a neighbourhood of the decision rule, termed switching function [9–11]. Furthermore, in some cases fuzzy control technique has been used to improve the control performance of the process where “if-then rules” are implemented according to the current situation of the system states [12, 13]. Nevertheless, nonlinear Model Predictive Control (NMPC) has shown very good performances in successful applications, especially in process industries, due to its high degree of robustness [14, 15]. In [14] three non-linear MPC Algorithms (nMPC, PIDnMPC and SnMPC) are developed to control fast systems and tested experimentally using a fabricated planar 2-link vertical robotic arm apparatus. Moreover, based on a nonlinear model predictive control approach and preserving closed loop stability, in [15] an online gait control scheme is proposed for control trajectory in biped robots. This work proposes a discrete-time Nonlinear MPC (DT-NMPC) technique in which a linearizing method is not required to present a good performance system control.

The paper is organized as follows: Sections 2 gives the preliminaries of feedback linearization control as a theoretical antecedent of nonlinear control systems. Section 3 presents the proposed finite dimensional discrete time NMPC. Section 4 considers two study cases: the single-link flexible joint control and the inverted pendulum control, in this section simulation results and performance comparisons of both techniques FLC and DT-NMPC in terms of overshoot and settling time are shown. Finally,

Manuscript received January 22, 2018; revised May 11, 2018; accepted June 10, 2018. Recommended by Associate Editor Changsun Ahn under the direction of Editor Young Il Lee. This work is supported by the Tecnologico de Monterrey and the National Council for Science and Technology (CONACYT), México. The authors also want to show great thanks to the research group of Sensors and Devices of the School of Engineering and Sciences for its support for the development of this work.

Carlos Sotelo, Antonio Favela-Contreras, Graciano Dieck-Assad, Pedro Rodríguez-Cañedo, and David Sotelo are with Tecnologico de Monterrey, Escuela de Ingenieria y Ciencias, México (e-mails: ing_carlossotelo@hotmail.com, antonio.favela@itesm.mx, graciano.dieck.assad@itesm.mx, rodriguezpedro1709@gmail.com, ing_davidsotelo@hotmail.com). Francisco Beltrán-Carbajal is with Universidad Autónoma Metropolitana, Unidad Azcapotzalco, Departamento de Energía, México (e-mail: fbeltran@azc.uam.mx).
* Corresponding author.

Section 5 discusses the conclusions.

2. FEEDBACK-LINEARIZATION CONTROL

This section presents a brief review of FLC. The original controller, proposed by Chen in [16], is based on the idea of feedback linearization, transforming the nonlinear system dynamics into a linear one, so linear control techniques can be applied [17].

When systems have the nonlinearity in the last state or just in one state, it is easy by inspection to cancel the nonlinearity and then apply linear control techniques [2]. However, if the model has nonlinearities in two or more states, it is not possible to perform the input-output linearization control. The idea of feedback linearization, i.e., of canceling the nonlinearities and imposing a desired linear dynamics, can be simply applied to a class of nonlinear state space model described by the so-called companion form. A nonlinear system is said to be in companion form if its dynamics is represented by

$$\begin{aligned} \dot{x} &= f(x) + g(x)u, \\ y &= h(x), \end{aligned} \tag{1}$$

where u is the scalar control input, x is the state vector, $h(x)$ is the scalar output of interest, and the vector fields $f(x)$ and $g(x)$ are nonlinear functions of the states. A system (1) is input-state linearizable if and only if:

- The rank $\left\{g, ad_f g, \ldots, ad_f^{\rho-1} g\right\} = \rho$, the vector fields are linearly independent in Ω
- The span $\left\{g, ad_f g, \ldots, ad_f^{\rho-2} g\right\}$ is involutive in Ω.

where $ad_f g$ stands for the Lie bracket of f and g, and ρ is the relative degree of the nonlinear system.

Looking for the linear state space model in canonical form, a coordinate transformation $T(\cdot)$, that must present diffeomorphism, is used to transform the state equation from the $x-$ coordinates to the $z-$ coordinates, where z_i must satisfies the following necessary conditions:

$$\frac{\partial z_i}{\partial x} g = L_g z_i = 0 \qquad i = 1, \ldots, (n-1), \tag{2}$$

$$\frac{\partial z_n}{\partial x} g = L_g z_n \neq 0, \tag{3}$$

where $z_1 = h(x)$ and $z_{i+1} = L_f z_i$ for $i = 1, \ldots, (n-1)$. Thus, the equivalent Linear State Space Model in canonical form is:

$$\dot{\mathbf{z}} = \mathbf{A}z + \mathbf{B}v,$$

$$\therefore \mathbf{z} = \begin{bmatrix} z_1 \\ z_2 \\ \vdots \\ z_n \end{bmatrix} = \begin{bmatrix} y \\ \dot{y} \\ \vdots \\ y^{(n-1)} \end{bmatrix} = \begin{bmatrix} h(x) \\ L_f h(x) \\ \vdots \\ L_f^{(n-1)} h(x) \end{bmatrix} = \begin{bmatrix} z_1 \\ L_f z_1 \\ \vdots \\ L_f^{(n-1)} z_1 \end{bmatrix},$$

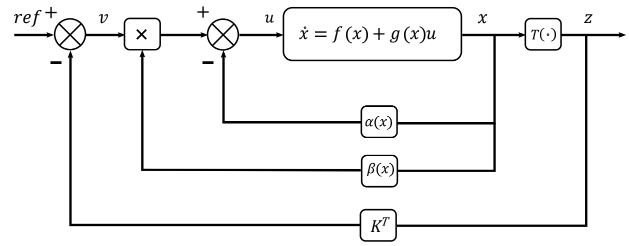

Fig. 1. Feedback linearization control block diagram.

$$\begin{bmatrix} \dot{z_1} \\ \dot{z_2} \\ \vdots \\ \dot{z}_{n-1} \\ \dot{z_n} \end{bmatrix} = \begin{bmatrix} 0 & 1 & 0 & 0 & \ldots & 0 & 0 \\ 0 & 0 & 1 & 0 & \ldots & 0 & 0 \\ \vdots & \vdots & \vdots & \vdots & \ddots & \vdots & \vdots \\ 0 & 0 & 0 & 0 & \ldots & 0 & 1 \\ 0 & 0 & 0 & 0 & \ldots & 0 & 0 \end{bmatrix} \begin{bmatrix} z_1 \\ z_2 \\ \vdots \\ z_{n-1} \\ z_n \end{bmatrix} + \begin{bmatrix} 0 \\ 0 \\ \vdots \\ 0 \\ 0 \end{bmatrix} v, \tag{4}$$

where $\dot{z_n} = L_f^{(n)} z_1 + L_g L_f^{(n-1)} z_1 \; u = v$ then the control law that linearize the system is:

$$\begin{aligned} u &= \alpha(x) + \beta(x) v, \\ u &= \frac{-L_f^{(n)} z_1}{L_g L_f^{(n-1)} z_1} + \frac{1}{L_g L_f^{(n-1)} z_1} v. \end{aligned} \tag{5}$$

Fig. 1 shows the Feedback Linearization Control (FLC) scheme. The diagram provides a clearer idea of how the system is first linearized and then controlled. The first part consists of calculating the inner loops parameters $\alpha(x)$ and $\beta(x)$. They generate the input u from (5) that linearizes the system. After the coordinates' transformation is complete, vector k provides the control input v that stabilizes the system at the reference.

3. DISCRETE-TIME NONLINEAR MODEL PREDICTIVE CONTROL

3.1. Introduction

Previous works have proposed to apply Nonlinear Model Predictive Control (NMPC) to continuous-time models. Recent work about this controller [9, 18] shows the NMPC application to a nonlinear synchronous motor and to a photovoltaic system. However, all the calculations are performed in continuous-time. Up to now discretization works of this controller have not been performed.

Currently, different predictive control techniques based on state-space models has been proposed [19–21]. Some NMPC, as we established previously, perform an online linearization and then apply control. Also, state-dependent Ricatti equation technique is employed to perform nonlinear control. It overcomes many of the difficulties of existing methods such as feedback linearization, and delivers computationally efficient algorithms.

This technique recast a nonlinear system's dynamics into a form resembling linear dynamics. State observers are used to enhance the controller robustness [22]. In this work the robustness of the proposed controller is tested during disturbances without the need of observers. The proposed controller has many advantages over conventional NMPCs, one of the most important is that is able to avoid the principal drawbacks that typical NMPC presents such as the optimization problem that is generally non-convex because the equations are nonlinear. Consequently, the problem of existence of an on-line solution of the nonlinear program is crucial one, possible local minima existence. Nominal stability is insured only when the prediction horizon is infinite.

NMPC can be applied when the system satisfies the following assumptions:

- The system has a relative degree well or ill defined.
- All states are available.
- Output and reference signals are sufficiently many times differentiable with respect to t.

This NMPC technique is based on concepts such as prediction via Taylor series, receding horizon control, quadratic cost function optimization and feedback linearization control.

3.2. Discrete-time NMPC (DT-NMPC) development

Considering the system model (1), it is proposed a finite dimensional discrete nonlinear equivalent system using a Backward Euler implicit scheme

$$\frac{x_i^k - x_i^{k-1}}{\Delta t} = f\left(x_i^k\right) + g\left(x_i^k\right) u_i^k, \qquad (6)$$
$$y_i^k = h\left(x_i^k\right),$$

where x_i^k stands for state variables, f, g and h are functions of the state variables, u_i^k the control input and y_i^k the output variable.

According to this representation and using a Backward scheme in space, Lie Derivative of h along trajectories of x can be computed for the given vector fields f and g. Assuming that the state variable $x(t)$ is known at all time, a predictive control law for nonlinear systems is defined.

For finite dimensional output prediction, Taylor series expansion (7) is used considering a fixed space.

$$y_i^{k+1} \cong h\left(x_i^k\right) + kL_f h\left(x_i^k\right) + \ldots + \frac{k^{(n)}}{n!}\left[L_f^{(n)} h\left(x_i^k\right) + L_g L_f^{(n-1)} h\left(x_i^k\right) u_i^k\right], \qquad (7)$$

where n is the order of the system. Then, writing (7) in a vector form and considering that $\mathrm{H} = L_g L_f^{(n-1)} h\left(x_i^k\right)$

$$y_i^{k+1} \cong T_y^{\mathrm{T}} Y_i^k, \qquad (8)$$

where

$$T_y = \begin{bmatrix} 1 & k & \ldots & \frac{k^n}{n!} \end{bmatrix}^{\mathrm{T}}, \qquad (9)$$
$$Y_i^k = \begin{bmatrix} h\left(x_i^k\right) & L_f h\left(x_i^k\right) & \ldots & L_f^{(n)} h\left(x_i^k\right) + \mathrm{H}\, u_i^k \end{bmatrix}^{\mathrm{T}}.$$

Thus, the output matrix Y_i^k can be written as follows:

$$Y_i^k = \begin{bmatrix} h(x) \\ L_f h(x) \\ \vdots \\ L_f^{(n)} h(x) \end{bmatrix} + \mathcal{H}\, u_i^k, \qquad (10)$$

where

$$\mathcal{H} = \begin{bmatrix} \mathbf{0}_{n\times 1} \\ \mathrm{H} \end{bmatrix}. \qquad (11)$$

To obtain the control law, the mathematical expression of the performance index (12) is defined:

$$J = \sum_{q=1}^{k_h} \left(y_i^{k+1} - w_i^{k+1}\right)^{\mathrm{T}} \left(y_i^{k+1} - w_i^{k+1}\right) + \sum_{q=1}^{k_h} \lambda u_i^{k\,\mathrm{T}} \bar{R} u_i^k, \qquad (12)$$

where k_h stands for the prediction horizon, and the tuning parameters for the manipulation are: $\bar{R}$ defined as a pondering matrix with dimension $n_u \times n_u$ where n_u corresponds to the number of control variables, and λ as a positive constant value that penalizes the large excursion of the control vector. Moreover, $y_i^{(k+1)}$ is the predicted output vector and $w_i^{(k+1)}$ is the predicted reference vector. In order to deal with the offset-free behavior, u_i^k is considered as a deviation variable defined as $\bar{u}_i^k - {u^d}_i^k$, where $\bar{u}_i^k$ stands for the input signal and ${u^d}_i^k$ corresponds to the steady-state control value which could be calculated as in [23] or set equal to 0 as in [24] when no specific value is available. As in (8), based on a Taylor series expansion and considering a fixed space for a finite dimensional representation, the predicted reference $w_i^{(k+1)}$ is expressed in the following vector form

$$w_i^{k+1} \cong T_y^{\mathrm{T}} W_i^k, \qquad (13)$$

where

$$W_i^k = \begin{bmatrix} w_i^k & \frac{w_i^k - w_i^{k-1}}{\Delta t} & \ldots & \left(\frac{w_i^k - w_i^{k-1}}{\Delta t}\right)^n \end{bmatrix}^{\mathrm{T}}. \qquad (14)$$

Using notations (10) and (14), (12) is rewritten as

$$J = k_h \left(T_y^{\mathrm{T}} Y_i^k - T_y^{\mathrm{T}} W_i^k\right)^{\mathrm{T}} \left(T_y^{\mathrm{T}} Y_i^k - T_y^{\mathrm{T}} W_i^k\right) + k_h \lambda u_i^{k\,\mathrm{T}} \bar{R} u_i^k. \qquad (15)$$

Factoring T_y^{T} in the first element of the sum

$$J = \left(Y_i^k - W_i^k\right)^{\mathrm{T}} k_h T_y T_y^{\mathrm{T}} \left(Y_i^k - W_i^k\right) + \lambda u_i^{k\,\mathrm{T}} k_h \bar{R} u_i^k. \qquad (16)$$

For simplicity, $T_y T_y^{\mathrm{T}} = T_{\hat{Y}}$ and $k_h \bar{R} = R$. Then, the cost function is expressed as shown in (17) where T_y is a tuning parameter defined as a constant value that is used to penalize the tracking error

$$J = \left(Y_i^k - W_i^k\right)^{\mathrm{T}} T_{\hat{Y}} \left(Y_i^k - W_i^k\right) + \lambda \left(u_i^k\right)^{\mathrm{T}} R \left(u_i^k\right). \quad (17)$$

For simplicity, a matrix $\mathcal{M}$ that contains de output error is proposed

$$\mathcal{M}_i^k = \begin{bmatrix} h\left(x_i^k\right) \\ L_f h\left(x_i^k\right) \\ \vdots \\ L_f^{(n)} h\left(x_i^k\right) \end{bmatrix} - \begin{bmatrix} w_i^k \\ \frac{w_i^k - w_i^{k-1}}{\Delta t} \\ \vdots \\ \left(\frac{w_i^k - w_i^{k-1}}{\Delta t}\right)^n \end{bmatrix}. \quad (18)$$

Using (11) and (18) in (17) the cost function to be minimized respect to $\bar{u}_i^k$ becomes

$$J = \left(\mathcal{M}_i^k + \mathcal{H} u_i^k\right)^{\mathrm{T}} T_{\hat{Y}} \left(\mathcal{M}_i^k + \mathcal{H} u_i^k\right) + \lambda \left(u_i^k\right)^{\mathrm{T}} R \left(u_i^k\right). \quad (19)$$

Then, the control law is obtained from (20) as:

$$u_i^k = -\left(\mathcal{H}^{\mathrm{T}} T_{\hat{Y}} \mathcal{H} + \lambda R\right)^{-1} \mathcal{H}^{\mathrm{T}} T_{\hat{Y}} \mathcal{M}_i^k. \quad (20)$$

Input-state and input-output feedback linearization control techniques are the basic idea of the nonlinear-MPC proposed by Chen [16]. In his work uses the mathematical tools studied in Section 2.A and 2.B. The idea of using these tools is to find a relation between the input and output system and then calculate the input u using NMPC. Unlike FLC that linearizes the system, DT-NMPC finds the optimal input by minimizing a cost function that considers and ponders the output error and the manipulation variable.

The controller is developed in continuous-time in [16]. One of the objectives of this paper is to discretize the NMPC using Euler's backwards method. Euler's is a first order method, easy to implement and that assures stability after discretization is performed.

4. SIMULATION AND RESULTS

4.1. Example 1: flexible-joint mechanism

The flexible joint mechanism corresponds to a nonlinear system with a difficult control problem. It refers to a link driven by a motor through a torsional spring in the vertical plane Fig. 2 where q_1 is the link angular position and q_2 is the motor torque. Similarly, components and variables such as the link mass M, the link length L, stiffness k, and the rotor inertia J are involved.

Consider the nonlinear system of a flexible-joint mechanism given in [3] where it is represented by a three order model. The equations of motion can be reduced in the

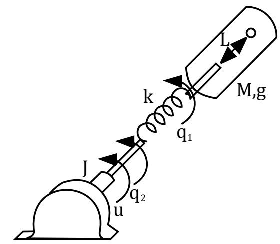

Fig. 2. Flexible joint mechanism.

Table 1. Single flexible-joint mechanism parameters.

Symbol	Parameter	Value
R	Electric Resistence	1 Ohm
L_{ind}	Electric Inductance	0.5 Henry
K_b	Electromotive Force Constant	0.01 V/[rad/s]
K_t	Motor Torque Constant	0.01 [N·m]/Amp
J	Moment of Inertia of the Rotor	0.01 kg·m^2
B	Motor Viscous Friction Constant	0.1 N·m·s

state-space model as:

$$\begin{cases} \dot{x}_1 = x_2, \\ \dot{x}_2 = -\mathfrak{d} \sin(x_1) - \mathfrak{e} x_2 + \mathfrak{f} x_3, \\ \dot{x}_3 = -\mathfrak{b} x_2 - \mathfrak{a} x_3 + \mathfrak{c} u, \\ y = x_1, \end{cases} \quad (21)$$

where x_1 is the link angular position q_1, x_2 is the link angular velocity $\dot{q}_1$, x_3 is the motor torque q_2, u is the control input, $\mathfrak{a} = R/L_{ind}$, $\mathfrak{b} = [K_b \cdot K_t]/L_{ind}$, $\mathfrak{c} = K_t/L_{ind}$, $\mathfrak{d} = MgL/J$, $\mathfrak{e} = B/J$ and $\mathfrak{f} = 1/J$, are positive constants, their parameters are shown in Table 1.

Based on FLC technique (21) is rerranged in the form of (1), thus (22) is obtained:

$$f(x) = \begin{bmatrix} x_2 \\ -\mathfrak{d} \sin(x_1) - \mathfrak{e} x_2 + \mathfrak{f} x_3 \\ -\mathfrak{b} x_2 - \mathfrak{a} x_3 \end{bmatrix}; \quad (22)$$

$$g(x) = \begin{bmatrix} 0 \\ 0 \\ \mathfrak{c} \end{bmatrix} u; \quad h(x) = x_1.$$

Considering the Relative Degree of the system is $\rho = 3$, the following steps are performed.

1) Construct the vector fields $g, ad_f g, ad_f^2 g$:

$$g = \begin{bmatrix} 0 & 0 & c \end{bmatrix}^{\mathrm{T}},$$
$$ad_f g = \begin{bmatrix} 0 & \mathfrak{f}\mathfrak{c} & -\mathfrak{a}\mathfrak{c} \end{bmatrix}^{\mathrm{T}},$$
$$ad_f^2 g = \begin{bmatrix} \mathfrak{f}\mathfrak{c} & -\mathfrak{e}\mathfrak{f}\mathfrak{c} - \mathfrak{a}\mathfrak{f}\mathfrak{c} & -\mathfrak{b}\mathfrak{f}\mathfrak{c} + \mathfrak{a}^2\mathfrak{c} \end{bmatrix}^{\mathrm{T}}.$$

2) Check controllability and involutivity conditions: Controllability matrix:

$$C = \begin{bmatrix} g & ad_f g & ad_f^2 g \end{bmatrix} \rightarrow det = \frac{c^3}{J^2} \neq 0,$$

C is controllable.

Involutivity matrix:

$$\left[\begin{array}{cc} g & ad_f g \end{array}\right] = \left[\begin{array}{cc} 0 & 0 \\ 0 & \mathfrak{f}\mathfrak{c} \\ \mathfrak{c} & -\mathfrak{a}\mathfrak{c} \end{array}\right] \neq \left[\begin{array}{cc} m & km \end{array}\right].$$

Vectors are constant, they form an involutive set. The result is not expressed as a linear combination k of the original set of vector fields.

3) Compute the state transformation z, based on the necessary conditions (2), (3) and the linear state space defined in (4)

$$\mathbf{z} = \left[\begin{array}{c} z_1 \\ z_2 \\ z_3 \end{array}\right] = \left[\begin{array}{c} x_1 \\ x_2 \\ -\mathfrak{d}\sin(x_1) - \mathfrak{e}(x_2) + \mathfrak{f}(x_3) \end{array}\right].$$

4) Compute the input transformation given by (5). Considering the Relative Degree of the system is $\rho = n = 3$, linearizing input u can be computed as follows:

$$u = \underbrace{\frac{-L_f^{(3)} z_1}{L_g L_f^{(2)} z_1}}_{\alpha(x)} + \underbrace{\frac{1}{L_g L_f^{(2)} z_1}}_{\beta(x)} v. \tag{23}$$

First, we compute $\alpha(x)$. The denominator is:

$$L_g L_f^{(2)} z_1 = L_g L_f z_2 = L_g z_3 = \frac{\partial z_3}{\partial x} g(x),$$
$$\therefore \frac{\partial z_3}{\partial x} = \left[\begin{array}{ccc} -\mathfrak{d}\cos(x_1) & -\mathfrak{e} & +\mathfrak{f} \end{array}\right].$$

Thus,

$$L_g L_f^{(2)} z_1 = \mathfrak{f}\mathfrak{c}.$$

Similarly, the numerator can be computed as follows:

$$L_f^{(3)} z_1 = L_f L_f^{(2)} z_1 = L_f L_f z_2 = L_f z_3 = \frac{\partial z_3}{\partial x} f(x).$$

Thus,

$$L_f^{(3)} z_1 = \mathfrak{d} x_2 \cos(x_1) + \mathfrak{e}[\mathfrak{d}\sin(x_1) + \mathfrak{e}x_2 - \mathfrak{f}x_3] + \mathfrak{f}[-\mathfrak{b}x_2 - \mathfrak{a}x_3].$$

By substituting in $\alpha(x)$,

$$\alpha(x) = \frac{MgL}{\mathfrak{c}} x_2 \cos(x_1) + \frac{B}{\mathfrak{c}}[-\mathfrak{d}\sin(x_1) - \mathfrak{e}x_2 + \mathfrak{f}x_3] + \frac{\mathfrak{b}}{\mathfrak{c}} x_2 + \frac{\mathfrak{a}}{\mathfrak{c}} x_3. \tag{24}$$

Then, we compute $\beta(x)$,

$$\beta(x) = \frac{J}{\mathfrak{c}} v \tag{25}$$

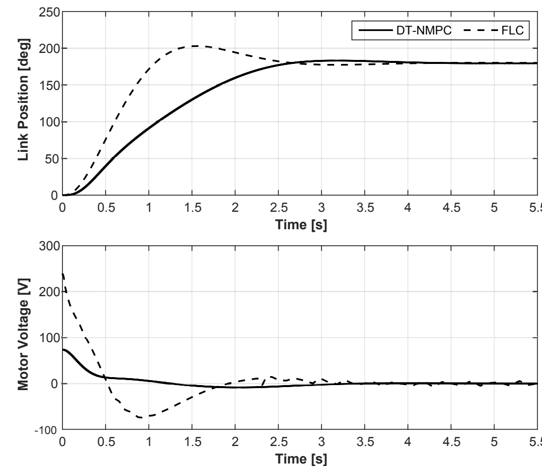

Fig. 3. Single-link flexible joint robot performance under DT-NMPC and FLC.

Based on (5), linearizing input u is as follows:

$$u = \frac{MgL}{\mathfrak{c}} x_2 \cos(x_1) + \frac{B}{\mathfrak{c}}[-\mathfrak{d}\sin(x_1) - \mathfrak{e}x_2 + \mathfrak{f}x_3] + \frac{\mathfrak{b}}{\mathfrak{c}} x_2 + \frac{\mathfrak{a}}{\mathfrak{c}} x_3 + \frac{J}{\mathfrak{c}} v. \tag{26}$$

The proposed tracking control law is

$$v = \dddot{x}_{1d} - k_0 e - k_1 \dot{e} - k_2 \ddot{e}, \tag{27}$$

where $e = x_1 - x_{1d}$ is the tracking error. Gains $K^{\mathrm{T}} = [k_0 \;\; k_1 \;\; k_2]$ are obtained using the following Bessel poles:

$$p = \left[\begin{array}{ccc} -5.009 & -3.967 + 3.784i & -3.967 - 3.784i \end{array}\right]^{\mathrm{T}}.$$

In order to perform pole placement control, Ackerman's formula provides the following vector gain:

$$K^{\mathrm{T}} = \left[\begin{array}{ccc} 150.569 & 69.799 & 12.943 \end{array}\right].$$

In dashed line, Fig. 3 presents the results of applying FLC technique.

Now, based on the proposed discrete-time NMPC (DT-NMPC) technique, the system (21) is discretized using a Backward Euler implicit scheme, thus (28) is obtained:

$$\begin{cases} \dfrac{x_{1i}^k - x_{1i}^{k-1}}{\Delta t} = x_{2i}^k, \\ \dfrac{x_{2i}^k - x_{2i}^{k-1}}{\Delta t} = -\mathfrak{d}\sin\left(x_{1i}^k\right) - \mathfrak{e}x_{2i}^k + \mathfrak{f}x_{3i}^k, \\ \dfrac{x_{3i}^k - x_{3i}^{k-1}}{\Delta t} = -\mathfrak{b}x_{2i}^k - \mathfrak{a}x_{3i}^k + \mathfrak{c}u_i^k, \\ y_i^k = x_{1i}^k. \end{cases} \tag{28}$$

Rearranging (28) in the form of (6), (29) is obtained:

$$f\left(x_i^k\right) = \left[\begin{array}{c} x_{2i}^k \\ -\mathfrak{d}\sin\left(x_{1i}^k\right) - \mathfrak{e}x_{2i}^k + \mathfrak{f}x_{3i}^k \\ -\mathfrak{b}x_{2i}^k - \mathfrak{a}x_{3i}^k \end{array}\right]; \tag{29}$$

$$g\left(x_i^k\right) = \begin{bmatrix} 0 \\ 0 \\ \mathfrak{c} \end{bmatrix} u; \quad h\left(x_i^k\right) = x_{1_i}^k.$$

Lie Derivatives are given by:

$$\begin{aligned}
L_f h\left(x_i^k\right) &= x_{2_i}^k, \\
L_f^2 h\left(x_i^k\right) &= -\mathfrak{d}\sin\left(x_{1_i}^k\right) - \mathfrak{e}x_{2_i}^k + \mathfrak{f}x_{3_i}^k, \\
L_f^3 h\left(x_i^k\right) &= \frac{-\mathfrak{d}\left[\sin\left(x_{1_i}^k\right) - \sin\left(x_{1_{i-1}}^k\right)\right]}{\Delta x_1} x_{2_i}^k \\
&\quad - \mathfrak{e}\left[-\mathfrak{d}\sin\left(x_{1_i}^k\right) - \mathfrak{e}x_{2_i}^k + \mathfrak{f}x_{3_i}^k\right] \\
&\quad + \mathfrak{f}\left[-\mathfrak{b}x_{2_i}^k - \mathfrak{a}x_{3_i}^k\right], \\
L_g L_f^2 h\left(x_i^k\right) &= \mathfrak{f}\mathfrak{c}.
\end{aligned}$$

Choosing the tuning parameters:

$$T_y = 0.88, \ \lambda = 0.032, \ k_h = 33, \ \bar{R} = 0.03.$$

Taking constants from Table 1. DT-NMPC vector are:

$$Y_i^k = \begin{bmatrix} 3.1342 \\ 44x10^{-4} \\ 13x10^{-4} \\ 312.87 \end{bmatrix}, \ \mathcal{H} = \begin{bmatrix} 0 \\ 0 \\ 0 \\ 2 \end{bmatrix}, \ W_i^k = \begin{bmatrix} 3.1416 \\ 0 \\ 0 \\ 0 \end{bmatrix},$$

$$T_{\hat{Y}} = \begin{bmatrix} 0.33 & 0.2904 & 0.1278 & 0.0375 \\ 0.2904 & 0.2556 & 0.1124 & 0.0330 \\ 0.1278 & 0.1124 & 0.0495 & 0.0145 \\ 0.0375 & 0.0330 & 0.0145 & 0.0043 \end{bmatrix}.$$

In solid line, Fig. 3 displays the results of a single-link flexible joint robot under DT-NMPC technique.

In order to observe the improvement of DT-NMPC over FLC technique applied to the single-link flexible joint robot, Fig. 3 presents the performance of the two control techniques. The top graph corresponds to the process variable while the bottom graph shows the manipulation variable. The set point of the angular position is 180° and the initial condition is zero. Fig. 3 shows that although the proposed DT-NMPC stabilizes the system slightly faster than FLC, using DT-NMPC the performance indexes are improved. DT-NMPC takes only 2.30 seconds while FLC reaches the desired position in 2.45 seconds as shown in Table 2. Additionally, DT-NMPC does not present overshoot while FLC has 12.8% of overshoot. On the other hand, FLC manipulation reaches 236 volts, an unrealistic value for a motor voltage, while DT-NMPC manipulation values are 75 volts. This is the principal disadvantage that presents FLC, it is not possible to penalize the increment of manipulated variable.

4.2. Example 2: inverted pendulum

The inverted pendulum is a nonlinear system with unstable dynamics where due to its fast time constants, it requires high bandwidth control. In this sense it is a difficult control problem which has been studied for years.

Table 2. Single flexible-joint mechanism controllers' performance comparison.

Control	Settling time	Overshoot	$\lvert u_{MAX}\rvert$
DT-NMPC	2.30 s	0 %	75 V
FLC	2.45 s	12.8 %	236 V

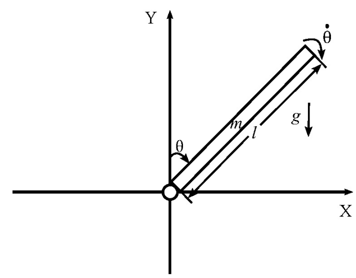

Fig. 4. Inverted pendulum.

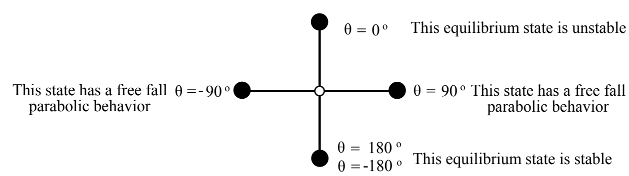

Fig. 5. Inverted pendulum operational regions.

The inverted pendulum refers to a two dimensional mechanical system where the axis of rotation is fastened - the pendulum rotates freely along its axis. Fig. 4 illustrates the inverted pendulum with its components and variables involved such as mass of the pendulum m, length of the pendulum l and gravity g including the acceleration a due to its single-axis movement and its angle of rotation θ.

Fig. 5 shows the inverted pendulum operational regions. The system inherently has two equilibria where only one of which is asymptotically stable. The asymptotically stable equilibrium corresponds to a state in which the pendulum is pointing downwards $\theta = 180°$. In the absence of any control force, the system will naturally return to this state. On the other hand, the unstable equilibrium corresponds to a state in which the pendulum points strictly upwards $\theta = 0°$ and, thus, requires a control force to maintain this position. Furthermore, between these equilibrium states $\theta = \pm 90°$, the inverted pendulum involves a free fall parabolic behavior. For this reason, starting from the stable equilibrium position $\theta = 180°$, the basic control objective is to maintain the unstable equilibrium position $\theta = 0°$ following a given trajectory with significantly nonlinear regions. Considering the nonlinear system of a simple pendulum given in [3]. The nonlinear state-space model is:

$$\begin{cases} \dot{x}_1 = x_2, \\ \dot{x}_2 = -\mathfrak{a}\left[\sin\left(x_1 + \delta\right) - \sin\left(\delta\right)\right] - \mathfrak{b}x_2 + \mathfrak{c}u, \\ y = x_1, \end{cases} \tag{30}$$

Table 3. Inverted pendulum parameters.

Symbol	Parameter	Value
f	Angular momentum	0.099 kg m^2/s
m	Mass of the pendulum	0.104 kg
l	Length of the pendulumu	0.980 m
g	Gravity	9.81 m/s^2

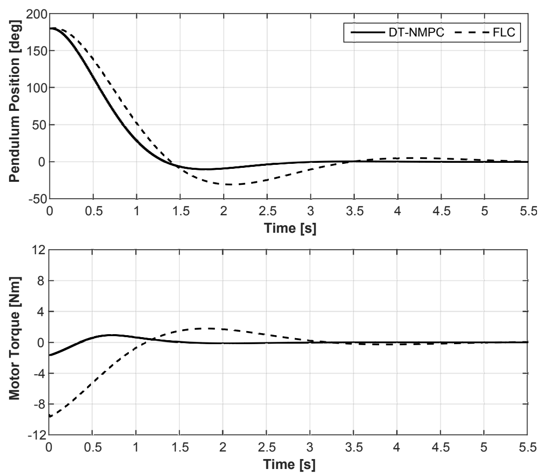

Fig. 6. Inverted pendulum performance under DT-NMPC and FLC.

where x_1 is the angular position θ, x_2 is the angular velocity $\dot{\theta}$, u is the control input, δ stands for the desired angular position ($\theta = 0°$), $\mathfrak{a} = g/l$, $\mathfrak{b} = f/ml^2$ and $\mathfrak{c} = 1/ml^2$ are positive constants, their parameters are shown in Table 3.

Considering that the Relative Degree of the system is $\rho = 2$ FLC technique is applied. By inspection of the state equations, it is possible to determine u that cancel the nonlinear term: $\mathfrak{a}[\sin(x_1+\delta) - \sin(\delta)]$.

$$u = \frac{\mathfrak{a}}{\mathfrak{b}}[\sin(x_1+\delta) - \sin(\delta)] + \frac{1}{\mathfrak{c}}v. \tag{31}$$

The tracking control law is:

$$v = k_1 x_1 + k_2 x_2. \tag{32}$$

Therefore, gains $K^{\mathrm{T}} = [k_1 \;\; k_2]$ are obtained using the following Bessel poles:

$$p = \begin{bmatrix} -4+4.59i & -4-4.59i \end{bmatrix}^{\mathrm{T}}.$$

In order to perform pole placement control, Ackerman's formula provides the following vector gain:

$$K^{\mathrm{T}} = -\begin{bmatrix} 3 & 0.7 \end{bmatrix}.$$

In dashed line, Fig. 6 presents the results of applying FLC technique.

Now, based on the proposed discrete-time NMPC (DT-NMPC) technique, the system (30) is discretized using a Backward Euler implicit scheme.Thus, the following discrete-time nonlinear state-space model [25] describes the inverted pendulum dynamics

$$\begin{cases} \dfrac{x_{1}{}_i^k - x_{1}{}_i^{k-1}}{\Delta t} = x_{2}{}_i^k, \\ \dfrac{x_{2}{}_i^k - x_{2}{}_i^{k-1}}{\Delta t} = -\mathfrak{a}\left[\sin\left(x_{1}{}_i^k + \delta\right) - \sin(\delta)\right] \\ \qquad\qquad - \mathfrak{b} x_{2}{}_i^k + \mathfrak{c} u_i^k, \\ y_i^k = x_{1}{}_i^k. \end{cases} \tag{33}$$

Rearranging (33) in the form of (6), (34) is obtained:

$$f\left(x_i^k\right) = \begin{bmatrix} x_{2}{}_i^k \\ -\mathfrak{a}\left[\sin\left(x_{1}{}_i^k + \delta\right) - \sin(\delta)\right] - \mathfrak{b} x_{2}{}_i^k \end{bmatrix};$$
$$g\left(x_i^k\right) = \begin{bmatrix} 0 \\ \mathfrak{c} \end{bmatrix} u; \;\; h\left(x_i^k\right) = x_{1}{}_i^k. \tag{34}$$

Lie derivatives are given by

$$L_f h\left(x_i^k\right) = x_{2}{}_i^k,$$
$$L_f^2 h\left(x_i^k\right) = -\mathfrak{a}\left[\sin\left(x_{1}{}_i^k + \delta\right) - \sin(\delta)\right] - \mathfrak{b} x_{2}{}_i^k,$$
$$L_g L_f h\left(x_i^k\right) = \mathfrak{c}.$$

Choosing the tuning parameters:

$$T_y = 0.6, \;\; \lambda = 0.02, \;\; k_h = 14, \;\; \bar{R} = 0.1.$$

NMPC vectors are given by:

$$Y_i^k = \begin{bmatrix} -5x10^{-4} \\ 6x10^{-4} \\ 43x10^{-4} \end{bmatrix}, \; \mathcal{H} = \begin{bmatrix} 0 \\ 0 \\ 10 \end{bmatrix}, \; W_i^k = \begin{bmatrix} 0 \\ 0 \\ 0 \end{bmatrix},$$
$$T_{\hat{Y}} = \begin{bmatrix} 0.14 & 0.0840 & 0.0252 \\ 0.0840 & 0.0504 & 0.0151 \\ 0.0252 & 0.0151 & 0.0045 \end{bmatrix}.$$

In solid line, Fig. 6 presents the simulation results of the DT-NMPC applied to the typical example of the inverted pendulum.

In order to show the improvement over a classical technique, this section contains a comparison between FLC and DT-NMPC applied to the inverted pendulum. Fig. 6 indicates the different control techniques responses. The top graph corresponds to the process variable while the bottom graph shows the manipulation variable. The initial position of the pendulum 180° (assuming the stable equilibrium point), and the reference is set to 0° (upright position). The two controllers show a similar performance, but it is important to consider that FLC uses the linearized model of the plant while DT-NMPC deals with all system nonlinearities. Fig. 6 shows that DT-NMPC stabilizes the system faster than FLC. DT-NMPC takes only 2.7 seconds to settle down while FLC reaches the zero in 5 seconds (Table 4). Moreover, DT-NMPC presents 5.58% of overshoot while FLC has 17.14% of overshoot. DT-NMPC and FLC present a maximum manipulation values of −1.6 and −9.4 Nm, respectively.

Table 4. Inverted Pendulum controllers' performance comparison.

Control	Settling time	Overshoot	$\lvert u_{MAX} \rvert$
DT-NMPC	2.7 s	5.58 %	1.6 Nm
FLC	5 s	17.14 %	9.4 Nm

5. CONCLUSIONS

This paper presents the design of a novel finite dimensional discrete-time NMPC (DT-NMPC). The concept of the Lie derivative is extended to the discrete time models, using Taylor series expansion and backward Euler's scheme in space and time to handle nonlinearities in well-known systems. Thus, introducing the algebraic definition of the Lie derivative, the proposed finite dimensional DT-NMPC is used to control and regulate the angular position in flexible joint and inverted pendulum as study cases.

Simulation results show that the proposed DT-NMPC structure stabilizes the nonlinear systems faster than the FLC technique. Using the proposed finite dimensional DT-NMPC, link position in flexible joint mechanism is achieved at its desired value, 180°, and pendulum position in inverted pendulum mechanism is maintained at 0° in spite of its initial value. Furthermore, in both study cases the outputs do not present a significant overshoot and the values of the manipulated variables are considerably lower than a commonly nonlinear control technique. In both examples, single-link flexible joint robot and the inverted pendulum controllers, settling times are either maintained about the same (from 2.45 to 2.30 s) or reduced drastically (from 5 to 2.7 s), for the FLC and DT-NMPC systems.

REFERENCES

[1] A. Isidori, *Nonlinear Control Systems*, Springer Science & Business Media, 2013.

[2] H. K. Khalil and J. Grizzle, *Nonlinear Systems*, vol. 3, Prentice-Hall, New Jersey, 2012.

[3] J.-J. E. Slotine and W. Li, *Applied Nonlinear Control*, vol. 199, no. 1, Prentice-Hall, Englewood Cliffs, NJ, 1991.

[4] X. Liu, W. Jiang, and X.-C. Dong, "Nonlinear adaptive control for dynamic and dead-zone uncertainties in robotic systems," *International Journal of Control, Automation, and Systems*, vol. 15, no. 2, pp. 875-882, 2017.

[5] Y. Shi, Y. Li, S. Li, and H. Liu, "State feedback design for nonlinear quadratic systems with randomly occurring actuator saturation," *International Journal of Control, Automation, and Systems*, vol. 15, no. 3, pp. 1117-1124, 2017.

[6] M. A. Mousavi, B. Moshiri, and Z. Heshmati, "A new predictive motion control of a planar vehicle under uncertainty via convex optimization," *International Journal of Control, Automation, and Systems*, vol. 15, no. 1, pp. 129-137, 2017.

[7] P. S. Gandhi, P. Borja, and R. Ortega, "Energy shaping control of an inverted flexible pendulum fixed to a cart," *Control Engineering Practice*, vol. 56, pp. 27-36, 2016.

[8] N. Van Chi, "Adaptive feedback linearization control for twin rotor multiple-input multiple-output system," *International Journal of Control, Automation, and Systems*, vol. 15, no. 3, pp. 1267-1274, 2017.

[9] R. Errouissi, J. Yang, W.-H. Chen, and A. Al-Durra, "Robust nonlinear generalised predictive control for a class of uncertain nonlinear systems via an integral sliding mode approach," *International Journal of Control*, vol. 89, no 8, pp. 1698-1710, 2016.

[10] N. P. K. Reddy, M. S. Kumar, and D. S. Rao, "Control of nonlinear inverted pendulum system using PID and fast Output sampling based discrete sliding mode controller," *International Journal of Engineering Research and Technology*, vol. 3, no. 10, pp. 1000-1006, 2014.

[11] M. Li and Y. Chen, "Sliding mode predictive tracking control for DC permanent magnet motor in NCSs with random delay and packet dropouts," *International Journal of Control, Automation, and Systems*, vol. 15, no. 6, pp. 2723-2732, 2017.

[12] Y. Qin, H. Peng, F. Zhou, X. Zeng, and J. Wu, "Nonlinear modeling and control approach to magnetic levitation ball system using functional weight RBF network-based state-dependent ARX model," *Journal of the Franklin Institute*, vol. 352, no. 10, pp. 4309-4338, 2015.

[13] A. Chakrabarty, S. Banerjee, S. Maity, and A. Chatterjee, "Fuzzy model predictive control of non-linear processes using convolution models and foraging algorithms," *Measurement*, vol. 46, no. 4, pp. 1616-1629, 2013.

[14] J. Wilson, M. Charest, and R. Dubay, "Non-linear model predictive control schemes with application on a 2 link vertical robot manipulator," *Robotics and Computer-Integrated Manufacturing*, vol. 41, pp. 23-30, 2016.

[15] R. Heydari and M. Farrokhi, "Robust model predictive control of biped robots with adaptive on-line gait generation," *International Journal of Control, Automation, and Systems*, vol. 15, no. 1, pp. 329-344, 2017.

[16] W.-H. Chen, D. J. Ballance, and P. J. Gawthrop, "Optimal control of nonlinear systems: a predictive control approach," *Automatica*, vol. 39, no. 4, pp. 633-641, 2003.

[17] S. Saxena and Y. V. Hote, "Internal model control based PID tuning using first-order filter," *International Journal of Control, Automation, and Systems*, vol. 15, no. 1, pp. 149-159, 2017.

[18] R. Errouissi, S. Muyeen, A. Al-Durra, and S. Leng, "Experimental validation of robust continuous nonlinear model predictive control based grid-interlinked photovoltaic inverter," *IEEE Transactions on Industrial Electronics*, vol. 63, no. 7, pp. 4495-4505, 2016.

[19] I. Chang and J. Bentsman, "Constrained discrete-time state-dependent Riccati equation technique: a model predictive control approach," *Proc. of 52nd IEEE Conference on Decision and Control*, pp. 5125-5130, 2013.

[20] G. A. Gonçalves and M. Guay, "Robust discrete-time set-based adaptive predictive control for nonlinear systems," *Journal of Process Control*, vol. 39, pp. 111-122, 2016.

[21] M. Lawryczuk, "Nonlinear statespace predictive control with online linearization and state estimation," *International Journal of Applied Mathematics and Computer Science*, vol. 25, no. 4, pp. 833-847, 2015.

[22] H. Salhi and F. Bouani, "Nonlinear parameters and state estimation for adaptive nonlinear model predictive control design," *Journal of Dynamic Systems, Measurement, and Control*, vol. 138, no. 4, p. 044502, 2016.

[23] S. K. Kim, D. K. Choi, K. B. Lee, and Y. I. Lee, "Offset-free model predictive control for the power control of three-phase AC/DC converters," *IEEE Transactions on Industrial Electronics*, vol. 62, no. 11, pp. 7114-7126, 2015.

[24] M. Alamir, *A Pragmatic Story of Model Predictive Control: Self-contained Algorithms and Case-studies*, CNRS-University of Grenoble, 2013.

[25] E. Ronco, T. Arsan, P. J. Gawthrop, and D. J. Hill, "Nonlinear continuous-time generalized predictive control through successive system linearisations," *Rapport technique EE-99005*, Laboratory for Dynamical Systems and Control, E&IE, Sydney, Australia, 1999.

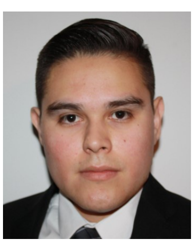

Carlos Sotelo received his B.S. in Mechatronics Engineering and his M.S. degree in Automation and Control Engineering, the two degrees from Tecnológico de Monterrey, Campus Monterrey, México, in 2010 and 2015, respectively. Furthermore, he has received his M.S. degree in Systems, Control and I&T from the Université Joseph Fourier of Grenoble, France in 2014. He is currently a PhD student ascribed in the Sensors and Devices research group at Tecnológico de Monterrey in Monterrey City. His main research interests are nonlinear control, mechatronics, parametric identification and predictive control of refinery processes.

Antonio Favela-Contreras received his B.S. and M.E. degrees in electronics and communications engineering and the M.S. degree in control engineering, all the three degrees from the Tecnológico de Monterrey, Campus Monterrey, México, in 1986, 1995 and 1991, respectively. In 1999 he received his Ph.D. degree in automatic control from the National Polytechnic Institute Institute of Grenoble, France. He has established industrial collaboration projects with Cementos Mexicanos (Cemex), Hojalata y Lámina (HYLSA), Vitro and PEMEX-Refinación, among others. He is a Professor in the Department of Mechatronics and Electrical, member of the Sensors and Devices Research Group at Tecnológico de Monterrey, member of the Mexican National Research System SNI-1 and member of the Mexican Academy of Science. His main research interests include adaptive and predictive control, control systems on a chip, analysis and control of hybrid systems, control of mechatronics systems and industrial process control.

Francisco Beltrán-Carbajal received his B.S. in Electromechanical Engineering from the Instituto Tecnologico de Zacatepec (México) and his Ph.D. in Electrical Engineering (Mechatronics) from the Centro de Investigación y Estudios Avanzados del Instituto Politecnico Nacional (CINVESTAV-IPN) in Mexico City. He is currently a Titular Professor in the Energy Department at Universidad Autónoma Metropolitana (UAM), Unidad Azcapotzalco in Mexico City. His main research interests are vibration control, rotating machinery, mechatronics, parametric identification and automatic control of electromechanical and electronic systems and industrial processes.

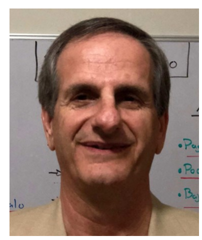

Graciano Dieck-Assad received his B.S. E.E. degree in Electronics and Communications Engineering at the Tecnológico de Monterrey in 1977. He received his M.S. and Ph.D. degrees from the University of Texas at Austin, in 1979 and 1984, respectively. He is the Associate Director of the Mechatronics, Electrical and Biomedical Engineering Department (MEBE) since 2017. He is ascribed to the sensors and devices group since 2000, and he teaches Microelectronics, Electromagnetic Fields and Bioinstrumentation at the Tecnológico de Monterrey since 1991.

Pedro Rodríguez-Cañedo received his B. Sc. Degree in electronic engineering form Instituto Tecnológico Nacional, Campus Culiacán in 2013, and his M.Sc. degree in electronic systems from Instituto Tecnológico y de Estudios Superiores de Monterrey in 2016. His research interests include industrial, nonlinear and predictive control.

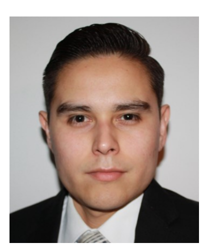

David Sotelo received his B.S. in Mechatronics Engineering and his M.S. degree in Automation and Control Engineering from Tecnológico de Monterrey, Campus Monterrey, México, in 2010 and 2015, respectively. Moreover, he has received the M.S. degree in Systems, Control and I&T from the Université Joseph Fourier of Grenoble, France in 2014. He is currently a Ph.D. student ascribed in the Sensors and Devices research group at Tecnológico de Monterrey in Monterrey City. His main research interests are optimal and robust control, process identification and design of control structures in crude oil distillation columns.